



Cite this: *Lab Chip*, 2023, 23, 1213

## Recent advances in microfluidics-based bioNMR analysis

Zheyu Li,<sup>ab</sup> Qingjia Bao,<sup>ab</sup> Chaoyang Liu,<sup>ab</sup> Ying Li,<sup>ib</sup> \*<sup>ab</sup>  
 Yunhuang Yang<sup>\*ab</sup> and Maili Liu<sup>ib</sup> <sup>ab</sup>

Received 22nd September 2022,  
 Accepted 1st December 2022

DOI: 10.1039/d2lc00876a

rsc.li/loc

Nuclear magnetic resonance (NMR) has been used in a variety of fields due to its powerful analytical capability. To facilitate biochemical NMR (bioNMR) analysis for samples with a limited mass, a number of integrated systems have been developed by coupling microfluidics and NMR. However, there are few review papers that summarize the recent advances in the development of microfluidics-based NMR ( $\mu$ NMR) systems. Herein, we review the advancements in  $\mu$ NMR systems built on high-field commercial instruments and low-field compact platforms. Specifically,  $\mu$ NMR platforms with three types of typical microcoils settled in the high-field NMR instruments will be discussed, followed by summarizing compact NMR systems and their applications in biomedical point-of-care testing. Finally, a conclusion and future prospects in the field of  $\mu$ NMR were given.

### 1. Introduction

Nuclear magnetic resonance (NMR) is a specific effect where certain atomic nuclei absorb and emit energy in a static magnetic field.<sup>1,2</sup> Measurement of the resonant energy exchange can provide detailed information about the properties of atomic nuclei and the structure,<sup>3</sup> dynamics<sup>4</sup> and chemical environment of molecules.<sup>5–7</sup> Consequently, NMR can be used to characterize many materials including solids and liquids, crystals and amorphous materials, and

<sup>a</sup> Key Laboratory of Magnetic Resonance in Biological Systems, State Key Laboratory of Magnetic Resonance and Atomic and Molecular Physics, National Center for Magnetic Resonance in Wuhan, Wuhan Institute of Physics and Mathematics, Innovation Academy for Precision Measurement Science and Technology-Wuhan National Laboratory for Optoelectronics, Chinese Academy of Sciences, Wuhan 430071, China. E-mail: liying@wipm.ac.cn, yang\_yh@apm.ac.cn  
<sup>b</sup> University of Chinese Academy of Sciences, Beijing 10049, China



**Zheyu Li**

microfluidics and NMR.

Zheyu Li received his bachelor's degree from College of Chemistry and Molecular Sciences at Wuhan University, and is pursuing his Ph.D degree in the Innovation Academy for Precision Measurement Science and Technology, CAS, China. His research projects focus on developing microfluidics-based mixers for studying fast folding kinetics of macromolecules, and he also has interest in developing technologies of combining



**Qingjia Bao**

Dr. Qingjia Bao received his Ph.D. in Physics from the Huazhong University of Science and Technology in 2013. Since then, his research has been focused on NMR&MRI instrument and methodology development. From 2007 to 2016, he developed several automatic shimming and data processing methods for the first high-field 500 MHz NMR spectroscopy in China. From 2016 to 2020, he developed an ultrafast method for diffusion and metabolism imaging. Now, he is a professor at the Innovation Academy for Precision Measurement Science and Technology, CAS, China. His research interest is developing new NMR/MRI instrumentation to explore new MR applications in analytical chemistry and metabolomics.

pure substances and mixtures.<sup>6,8</sup> Currently, this technology has made a profound impact on a wide range of fields such as chemistry,<sup>9,10</sup> biology,<sup>11</sup> medicine,<sup>12</sup> agriculture<sup>13</sup> and industry.<sup>14</sup> Among these research fields, biochemical NMR (bioNMR) is a major part of NMR studies. It has been playing an important role in molecular structure analysis,<sup>3,11</sup> proteomics<sup>15</sup> and metabolomics,<sup>16,17</sup> biomarker detection,<sup>18</sup> and *in vivo* imaging.<sup>19</sup> BioNMR has attracted wide attention due to its unique features, *e.g.*, label-free detection,<sup>20</sup> non-invasive analysis,<sup>21</sup> atomic-resolution determination,<sup>22</sup> and *in situ* characterization.<sup>20,22</sup>

As we know, the quality of NMR signals heavily relies on the three key components: a magnet, coil and radiofrequency (RF) transceiver.<sup>23</sup> The magnet produces a constant magnetic field to polarize nuclear spins, while the coil and RF transceiver transmit RF energy to the subject and receive the returning signal. Since NMR analysis significantly depends on a homogeneous and strong magnetic field to achieve a high sensitivity and resolution, most NMR experiments are

carried out on a bulky system and they often require a sample volume of up to hundreds of microliters at a millimole concentration scale.<sup>11</sup> This inevitably brings some contradictions in bioNMR analysis because biological samples often have a limited mass, *i.e.*, a limited volume down to a few microliters and relatively low concentration down to  $\mu\text{M}$ .<sup>24</sup> To address these contradictions, it is necessary to perform miniaturization for bioNMR systems.

As a direct way, the miniaturization in NMR analysis can be realized by using a small-size NMR tube with a capacity of several microliters to save precious samples.<sup>25,26</sup> Other attempts were also reported to further decrease the sample consumption, *e.g.*, using a capillary to load the sample and implementing home-made small coils to transfer the RF signal.<sup>27</sup> This strategy allows NMR analysis of nanomole samples in nanoliter volume. However, the sample should have very high concentrations (*e.g.*, tens of millimoles), which might limit its application in the analysis of low-solubility compounds or samples with low concentrations (smaller



**Chaoyang Liu**

*Dr. Chaoyang Liu is a professor at the Innovation Academy for Precision Measurement Science and Technology, CAS, China. He has long been committed to the research for developing magnetic resonance instruments and related applications, especially in the field of low-field and DNP-enhanced instruments recently. His team is developing a new MR system for both NMR spectroscopy and preclinical MRI.*



**Ying Li**

*Dr. Ying Li obtained his Ph.D. degree from the Huazhong University of Science and Technology in 2013. Subsequently, he received postdoctoral training at Houston Methodist Research Institute and Duke University from 2013 to 2018. He is now a Professor of the Innovation Academy for Precision Measurement Science and Technology, CAS, China. Dr. Li has rich experience in microfluidics-based bioanalysis and analytical chemistry. His research interest includes developing portable microfluidic platforms with CRISPR technology for biomarker detection and establishing integrated microfluidics-NMR systems for biomedical analysis.*



**Yunhuang Yang**

*Dr. Yunhuang Yang obtained his Ph.D. degree in radio physics from the Wuhan Institute of Physics and Mathematics, CAS, China, in 2005. He is currently a Professor and Principal Investigator at the Innovation Academy for Precision Measurement Science and Technology, CAS, China, with research interest in biological macromolecule structures and functions.*



**Maili Liu**

*Dr. Maili Liu is a Chief Scientist and Distinguished Professor at the Innovation Academy for Precision Measurement Science and Technology, CAS, China. His research interest includes development of novel NMR methodologies and applications for studying biomolecular structures and interactions.*

detectors do have better mass sensitivity than normal larger detectors, but small sample volumes with low concentrations result in a significant reduction in the number of spins and it will be difficult to obtain high quality NMR spectral data). In addition, the capillary can only “hold” the sample and cannot really “process” the sample, while biochemical samples often require some pretreatment (e.g., mix, isolate, concentrate) before the analysis.<sup>28</sup> To process minimal samples, a microfluidic platform or Micro Total Analysis System ( $\mu$ TAS) has been proposed and developed.  $\mu$ TAS has unique advantages in fluid control and device miniaturization.<sup>29,30</sup>  $\mu$ TAS often comprises microchannel networks, reservoirs, microvalves and other functional units.<sup>31</sup> It can also be integrated with electromechanical components<sup>32</sup> to realize automatic and high-throughput control of liquids,<sup>33</sup> cells<sup>34</sup> or even organisms.<sup>35</sup> Since  $\mu$ TAS has the capability to continuously handle nanoliter to microliter fluids, it should be promising to combine  $\mu$ TAS and NMR to form microfluidics-based NMR ( $\mu$ NMR) systems for the analysis of biochemical samples.

Currently, there are two main ways to establish  $\mu$ NMR systems based on microfluidics and NMR. The first one is to use a commercial high-field and high-resolution NMR instrument, and introduce a microfluidic chip (microchip) for sampling.<sup>36</sup> Since the microchip dimension does not fit a common NMR probe, proper designing should be proposed to match the microchip with the coil/probe, and especially ensure an acceptable detection sensitivity because less sample within microchannels would worsen the signal-to-noise ratio (SNR).<sup>37,38</sup> This type of  $\mu$ NMR system could perform NMR spectroscopy to analyze biochemical samples, or even study the intermediate products of dynamic reactions.<sup>39</sup> The second way to develop a microchip-based  $\mu$ NMR system is to use a home-made compact NMR system that is established on a portable low-field permanent magnet with an open and flexible sampling zone. Such a system allows a microchip to be conveniently mounted for parallel and sequential sample pretreatment,<sup>29</sup> though it also requires an appropriate arrangement of the coils, the circuits, the chip, the magnet and others, especially in the situation for multiplexed detection.<sup>40,41</sup> Compact  $\mu$ NMR platforms are suitable to perform NMR relaxometry (in contrast to NMR spectroscopy) to measure biomarkers in a fluid or on a cell membrane.<sup>42</sup> They might not be suitable for spectroscopy analysis due to the weak static fields, but they provide a means to perform fast and low-cost detection for biological samples based on NMR.

Indeed, a number of recent literature reports have shown promising studies on the above two types of  $\mu$ NMR systems. In this review, we mainly provide an overview of recent advances in the direct combination of microfluidic devices and NMR for bioNMR analysis. For more broad or other specific topics relevant to miniaturized NMR systems and applications, the readers can refer to other reviews<sup>39,42–45</sup> or books.<sup>46,47</sup> This review is organized as: section 2 providing the recent progress in  $\mu$ NMR based on state-of-the-art high-

field NMR instruments; section 3 reviewing compact  $\mu$ NMR platforms; section 4 providing a conclusion and proposing some possible directions in  $\mu$ NMR-based analysis in the future (Fig. 1).

## 2. $\mu$ NMR based on high-field commercial instruments

The introduction of microchips makes it difficult to use the saddleback-shaped RF coil of a common probe, which is settled in most commercial high-field NMR instruments. Therefore, it is necessary to modify the coil/probe to fit the microchip and also maintain or even increase the sensitivity. Researchers have made many attempts to adapt the coil forms to microdevices, including solenoid,<sup>27</sup> planar spiral<sup>51</sup> and stripline coils.<sup>52</sup> This section mainly summarizes recently developed  $\mu$ NMR platforms with the three types of microcoils based on the high-field NMR instruments.

### 2.1 Solenoid microcoil-based $\mu$ NMR

The solenoid coil is the most common electrical component for producing electromagnetic induction, and shows a great performance in converting electric fields to magnetic fields.<sup>53</sup> It has been widely used for making microcoils due to the uniform magnetic field within the coil (Fig. 2Ai).<sup>27</sup> As an initial attempt to introduce microfluidics to commercial NMR instruments, McDonnell *et al.* implemented a commercial imaging NMR probe with a large enough diameter to encompass the entire microfluidic device.<sup>54</sup> They further optimized the probe and integrated a device for remote NMR detection and imaging.<sup>55</sup> These studies demonstrated the possibility of combining microfluidics and NMR, but they did not really explore the unique function of microfluidics. To take advantage of microchips, Meier *et al.* presented an integrated microfluidic device for on-chip NMR studies (Fig. 2Aii).<sup>56</sup> By utilizing the precise liquid controlling ability of the microfluidic network, they obtained the NMR spectra of 20 nL pure deionized (DI) water and the magnetic resonance image (MRI) of gold nanoparticles (NPs) in a 150  $\mu$ m-wide microchannel. To increase the detection sensitivity, Mompeán *et al.* presented a method to perform photochemically induced dynamic nuclear polarization (photo-CIDNP) in solenoidal microcoil setups by introducing a microfluidic chip (Fig. 2Aiii).<sup>57</sup> This microchip consists of a double-inlet Y-shaped channel with the outlet channel encompassed by a solenoid microcoil. The transparent structure of the microchip allowed efficient irradiation of a photosensitizer by a laser beam. The microchip also enabled rapid and efficient mixing of two samples (e.g., *N*-acetyl-L-tyrosine and  $\beta$ -cyclodextrin) prior to irradiation and detection. The authors successfully monitored the <sup>1</sup>H resonance of the Tyr moiety under two different chemical conditions, proving that CIDNP could be used to non-invasively monitor the solvent accessibility of aromatic residues in peptides or proteins. Furthermore, their results





**Fig. 1** The overall concept of  $\mu$ NMR for bioNMR analysis. Microfluidics and NMR have their own specific features. Two main ways that could be used to integrate microfluidics and NMR into  $\mu$ NMR, are to modify the coil to allow microchips to match the high-field NMR systems, or to settle microchips on compact NMR systems with a small magnet and integrated circuits. These two types of  $\mu$ NMR systems can be used in various applications in chemistry, biology, medicine, and other fields.<sup>48–50</sup> Reproduced with permission from ref. 48. Copyright 2017 IEEE, ref. 49. Copyright 2021 Nature Publishing Group, and ref. 50. Copyright 2016 RSC publishing.

also demonstrated that the microchip-CIDNP-based strategy achieved a dramatic enhancement of the target sample's NMR signal and boosted the NMR detection down to a sub-picomole detection limit.

As discussed above, a solenoid RF coil is efficient in producing a homogeneous  $B_1$  field for samples located in the center of the coil. Meanwhile, the sampling zone could be very close to the coil, which is also beneficial to the detection sensitivity. However, for the same reason that the sample needs to be placed inside the solenoid (*e.g.*, in the form of pipes), the microfluidic devices and the solenoid RF coil often need to be manufactured on the same chip, resulting in a significant limitation in the designing and fabrication of the microchips. Moreover, complex microfluidic chips are generally made of polydimethylsiloxane (PDMS) or other plastics, which can cause a very strong  $^1\text{H}$  background signal due to the methyl groups ( $-\text{CH}_3$ ), and bring serious interference in spectra interpretation.

## 2.2 Planar spiral microcoil-based $\mu$ NMR

Another widely used form of microcoil in microfluidics-based NMR probes is the planar spiral coil.<sup>51</sup> This coil could be

regarded as a variant of the solenoid coil compressed to a flat surface and thus has the advantage of ease of integration with a flat circuit board.<sup>58</sup> A planar solenoid coil was first applied to micro-manufacturing in NMR by Massin *et al.*<sup>51</sup> The microcoil was processed on a glass plate by micro etching technology, and the  $^1\text{H}$  spectra of nanoliter-level samples in glass microwells were obtained on a 300 MHz NMR instrument. The authors found that the mean mass sensitivity of the microcoil was enhanced  $>100$  times that obtained in a 5 mm spinning tube for arginine and sucrose. This microscale NMR demonstrates the ability to acquire high-resolution spectra on several nanoliter samples with improved mass sensitivity, which could enable a variety of uses in biological applications.

To develop a microfluidics-based NMR probe, Fratila *et al.* proposed a non-resonant planar transceiver microcoil integrated in a microchip (sampling volume: 25 nL) that could detect different nuclides in the full broad-band range of Larmor frequencies (Fig. 2Bi).<sup>58</sup> The microchip can control the sample temperature by the heat exchange of the liquid in parallel adjacent winding channels. On this system, the detection of 1D and 2D spectra and homo- and heteronuclear experiments of  $^1\text{H}$ ,  $^{13}\text{C}$ ,  $^{19}\text{F}$  and  $^{31}\text{P}$  were completed. Since it



**Fig. 2** Solenoid microcoils and planar spiral microcoils and their applications. (A) The produced magnetic field ( $B_1$ ) of a typical solenoid microcoil with the sample (yellow area) located in the center, and the static magnetic field ( $B_0$ ) in a vertical direction. (i) A typical microcoil with a capillary for sampling.<sup>27</sup> (ii) Schematic illustration of the concept showing the solenoid microcoil surrounding a microchannel.<sup>56</sup> (iii) System setup for the DNP-based  $\mu$ NMR system.<sup>57</sup> (B) Planar spiral microcoil (blue) with the sample (yellow) loaded parallelly.  $B_0$  and  $B_1$  were indicated. (i) Design and images of the multipurpose NMR chip.<sup>58</sup> (ii) Top view of the microfluidic chip design of the 3D cell culture system, and the optical image with the microcoil superimposed onto the microchamber.<sup>59</sup> Reproduced with permission from ref. 27. Copyright 2014 AAAS, ref. 56. Copyright 2014 IOPscience, ref. 57. Copyright 2018 Fratila *et al.*, ref. 58. Copyright 2014 Esteve *et al.* and ref. 59. Copyright AIP publishing.

is hard for broad-band operation to precisely tune individual nuclei, the obtained spectral sensitivity might not reach the same level as those achieved in common NMR detectors. The introduction of more complicated microfluidics on  $\mu$ NMR was demonstrated by Esteve *et al.*, who presented a new microfluidic cell culture device compatible with real-time NMR.<sup>59</sup> The device realized capture, immobilization, and culture of cells, and its integration with a fiber-optic-based sensor allowed the measurement of oxygen, pH, and temperature during NMR monitoring (Fig. 2Bii). The collected NMR spectra of the 8 nL sample inside the microchip showed an accumulation of lactate and lipids when the neurosphere cultures were under anoxic conditions. In order to improve the resolution and SNR of the NMR spectra, Bordonali *et al.* introduced parahydrogen induced hyperpolarization (PHIP) into a  $\mu$ NMR platform.<sup>60</sup> This platform reduced the sample quantity and demonstrated high-field NMR chemosensing by applying Signal Amplification by Reversible Exchange (SABRE) in a PDMS membrane alveolus, which provided bubble-free hydrogen gas contact. This platform allowed NMR chemosensing of nanoliter detection volumes and micromolar concentrations corresponding to picomole molecular sensitivity.

Another typical form of planar spiral coil-based  $\mu$ NMR is that combined with digital microfluidics (DMF). DMF is a type of droplet microfluidics and can control the droplets individually by modifying the surface tension with an electrode array.<sup>61,62</sup> More specifically, DMF can precisely handle droplets on flat hydrophobic layers, which exactly matches the shape of a planar spiral coil. It is also very convenient for DMF to transport the sample droplet precisely to the center of the coil's sampling area for generating better signals. Swyer *et al.* introduced a two-plate DMF strategy to the interface small-volume samples with a planar spiral microcoil. In this system, the microcoil was surrounded by a copper plane that serves as the counter-electrode for the DMF device, allowing for precise control of the droplet position and shape.<sup>63</sup> They further achieved moving, splitting, merging and mixing of droplets on the DMF device and presented a load-shim-mix-measure process on the DMF-NMR.<sup>64</sup> As a result, they successfully monitored rapid organic reactions in organic solvents (*i.e.*, cyclohexene carbonate hydrolysis in dimethylformamide and a Knoevenagel condensation in methanol/water).

Due to the ease of fabrication of a planar spiral coil by micro etching, and the convenience of joining plane circuits and microchips,  $\mu$ NMR studies using a flat spiral coil can be extended to more applications, including 3D cell culture and *in situ* monitoring of cell responses to stimuli on a microfluidic chip with more complicated networks and functions.<sup>59</sup> Additionally, the planar coil-based  $\mu$ NMR platform also offers favorable means for parallel detection of multiple targets.<sup>58</sup> However, the limitation of the planar spiral coil is also apparent: its excitation field is not homogeneous and the field strength is not as strong as that of the solenoid coil, which can greatly impair the detection

sensitivity and is even worse for small volume samples. Meanwhile, like the situation of solenoid coils, the problem of  $^1\text{H}$  signal interference of plastics (*e.g.*, PDMS) still remains to be solved. This dilemma brings a question if there is a type of microcoil that could both excite a good excitation field and be integrated easily with microfluidic devices.

### 2.3 Stripline coil-based $\mu$ NMR

Stripline is a new type of microcoil that was developed to overcome the problems encountered with planar spiral microcoils (*e.g.*, inhomogeneous  $B_1$  field, static field distortions) and solenoid microcoils (*e.g.*, hard to fit the microchip).<sup>39</sup> The stripline configuration is often designed as a double tuned H/X and fabricated through lithographic methods (Fig. 3A).<sup>52</sup> In a stripline, the current is fed through a thin metal strip that is sandwiched between two ground planes placed above and below the strip, which can produce parallel field lines to the plane surface and thus result in a homogenous  $B_1$  field and great sensitivity comparable or better than that of a solenoid microcoil. Additionally, the design of a stripline probe is flexible and the dimension can be tuned according to the sample geometry. Bentum *et al.* first developed a  $\mu$ NMR system with a stripline coil that can collect  $^1\text{H}$  spectra.<sup>52</sup> After the chip was adapted with the probe, it could control the liquid at a flow rate of  $0.54\ \mu\text{L}\ \text{min}^{-1}$ , and could collect the high-resolution  $^1\text{H}$  spectrum of 600 nL samples. They further improved the stripline coil by integrating the coil and microfluidic chip detection part into a five-layer chip device.<sup>65</sup> The probe can distinguish multiple peaks with a half peak width of 0.7 Hz, and can also complete the acquisition of the  $^1\text{H}$ - $^1\text{H}$  COSY 2D spectrum.

To enable the dual-channel (*i.e.*,  $^1\text{H}$  and  $^{13}\text{C}$ ) measurement of mass-limited compounds, Kentgens and co-workers developed a HX stripline probe, by which they performed common  $^1\text{H}$ ,  $^{13}\text{C}$ , and heteronuclear NMR experiments for solutions such as ethyl crotonate and menthol under continuous flow.<sup>66</sup> Thereafter, this group improved the stripline-based  $\mu$ NMR platform by adding the shimming components to obtain a more homogenous magnetic field (Fig. 3B).<sup>67</sup> Furthermore, they demonstrated that they can monitor the acetylation of benzyl alcohol in the presence of *N,N*-diisopropylethylamine (DIPEA) by NMR from 1.5 s to several minutes, by employing a microfluidic stripline probe with a 150 nL detection volume.<sup>68</sup> Kentgens' group also proposed a split-contact stripline to further improve the resolution of NMR spectra.<sup>69</sup>

Though the stripline-based probe is powerful for analyzing low-mass samples, it requires a careful arrangement of the microfluidic device to match the sample with the detection zone. To address this issue, Utz's group optimized the stripline configuration that was designed with a slit, in which a microfluidic device can be directly inserted (Fig. 3C).<sup>70</sup> By using this slit-based design, it is convenient to replace the microchip with different networks on the same probe. Importantly, the functional



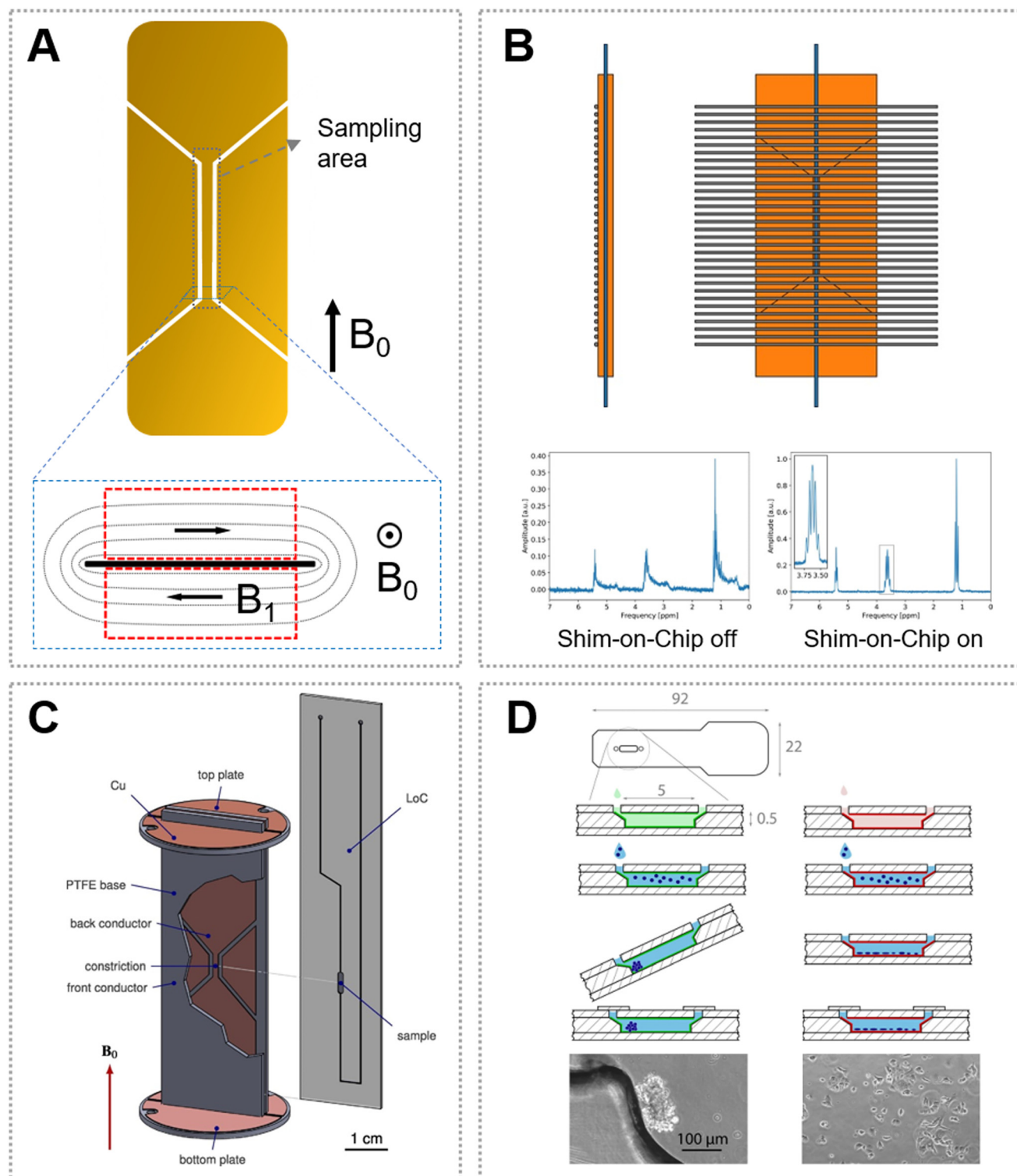


**Fig. 3** Stripline coil and its applications. (A) A typical stripline coil design. The inset shows the produced magnetic field distribution ( $B_1$ ) in a static magnetic field ( $B_0$ ). (B) Schematic of the shim-on-chip design of the stripline coil and calculated strength in the plane perpendicular to the parallel wires.<sup>67</sup> (C) A stripline with a slit for microchip insertion.<sup>70</sup> (D) Chip design and sample preparation for time-resolved non-invasive metabolomic monitoring of a single cancer spheroid in a stripline probe.<sup>72</sup> Reproduced with permission from ref. 67. Copyright 2018 ACS publications, ref. 70. Copyright 2016 Elsevier, and ref. 72. Copyright 2021 Nature Publishing Group.

microchannels (*e.g.*, for mixing and isolation) can be organized at one end of the device without inserting into

the slit, solving the problem of  $^1\text{H}$  signal interference from the PDMS materials.<sup>71</sup> With these promising characteristics,

this type of stripline probe was subsequently widely used in  $\mu$ NMR-based analysis.

By using the slit-based stripline, Marcel Utz and co-workers developed a cell-culture device that can be directly inserted into the NMR spectrometer probe.<sup>50</sup> The device allowed gas exchange during the cell culture by using a PDMS membrane attached to a PMMA chip, but the authors spatially separated the PDMS part from the NMR sampling area considering the strong background signals arising from the methyl groups. The oxygen permeation of the device was evaluated based on *in situ* NMR spectroscopy, showing that it can supply enough oxygen to maintain normoxic conditions for 10 000 MCF-7 cells. Furthermore, the authors increased the detection sensitivity of their  $\mu$ NMR platform, and quantitatively characterized the metabolic activity of a single spheroid culture of human cancer cells (*i.e.*, the consumption of D-glucose and production of L-lactic acid) (Fig. 3D).<sup>72</sup> Next, this research group updated the stripline-based system and developed a new microfluidic device for observing continuous mixing experiments.<sup>73</sup> Pneumatic microvalves were introduced into the microchip to control the liquid flow and mixing. The system allows injection of aliquots and *in situ* mixing of a chemical sample with <10  $\mu$ L volume, which was verified by using  $^1\text{H}$  spectroscopy. The sample volume could even be decreased, though it may require increasing the concentrations of the analytes considering the NMR detection limit. Such a stripline-based  $\mu$ NMR can also be used to study supramolecular processes.<sup>74</sup> The kinetic intermediates and rate-determining steps during the supramolecular reactions were determined, which are usually impossible to characterize by other analytical techniques.<sup>75</sup> Actually, the stripline-based  $\mu$ NMR can also be integrated with hyperpolarization techniques to increase the detection sensitivity. For example, PHIP was implemented in a microchip for the quantification of the kinetics and yield of [ $^{13}\text{C}$ ]fumarate from [ $^{13}\text{C}$ ]disodium acetylene dicarboxylate by NMR, though its use in a biological system requires further optimization.<sup>76</sup>

As a new NMR detector mode, the stripline coil meets both the need for sensitivity and integration with microfluidic chips. As a result, stripline coil-based  $\mu$ NMR not only allows the spectrum-based detection of nanoliter chemical samples, but also provides an efficient way to characterize cell properties, supramolecular dynamics and hyperpolarization. The limitation of the stripline coil is its capability for multiplexed sample detection, though further attempts could solve this issue.

### 3. $\mu$ NMR based on low-field compact platforms

In recent years, NMR has also been widely used in the field of biomolecular detection.<sup>77,78</sup> Compact NMR platforms that use small permanent magnets have further promoted the point-of-care testing (POCT) in biomedical applications.<sup>29,79</sup> The compact systems are convenient to be integrated with

microfluidics since they provide an open access for sampling.<sup>80–82</sup> However, their detection sensitivity and resolution are relatively low for spectroscopy analysis due to the weak and inhomogeneous magnet field. In contrast, this type of  $\mu$ NMR system is promising for biomarker detection based on relaxometry analysis, showing advantages of low background, low sample consumption, minimum sample preparation, rapid analysis time, convenient readout, and high specificity and sensitivity. Relaxometry measurements using the  $\mu$ NMR system often use labelled magnetic nanoparticles (MNPs) as the sensor, which was pioneered by Weissleder's group. MNPs create local magnetic fields when placed in NMR magnetic fields, and this can change the relaxation rate of adjacent water protons. The labelled MNPs can aggregate after recognizing the target biomarkers, and thus become more efficient at dephasing the spins of surrounding water molecules and significantly enhance spin-spin relaxation times ( $T_2$ ).<sup>83–85</sup> Based on this phenomenon, considerable progress has been achieved in the detection of various targets, including DNAs, proteins, pathogens and tumor cells.<sup>86</sup> We summarize the studies performed on compact  $\mu$ NMR systems with common channel microfluidics and digital microfluidics for sampling.

Weissleder's group first developed a handheld  $\mu$ NMR system for multiplexed, quantitative and rapid analysis of biological samples.<sup>40</sup> The system consists of four key parts: microcoils, on-board NMR electronics, a microfluidic chip, and a small permanent magnet. The microchip realized the effective mixing of different fluids, and partitioned the sample into multiple parts and delivered them to different microcoils. The radius and the height of the microchamber were optimized to allow the sample in close proximity to the planar coil to obtain a great filling factor. This system realized simultaneous detection of up to 8 protein biomarkers and achieved a great sensitivity (*e.g.*,  $1 \times 10^{-12}$  M) relying on the significant change of  $T_2$  caused by the association/disassociation of the labelled MNPs, which meant that its sensitivity can be similar or superior to enzyme-linked immunosorbent assay (ELISA). Furthermore, this group updated their  $\mu$ NMR system with an integrated probe that contains the solenoid microcoils and microfluidic channels, which resulted in >350% enhancement in the NMR signal compared to their previous system.<sup>87</sup> They detected as few as two cancer cells in a 1  $\mu$ L non-purified tumor sample based on the expression of the growth factor. Using a similar strategy, this research group analyzed 70 samples from tumor patients using a four-protein signature, achieving a 96% accuracy for cancer diagnosis.<sup>41</sup> Additionally, they designed a microchip with multiple functions (microvalves for fluid controlling, a filtering membrane for MNP isolation, and a herringbone mixer for fluid mixing) and integrated it with their  $\mu$ NMR system for profiling circulating microvesicles (MVs) from blood samples of glioblastoma patients (Fig. 4B).<sup>88</sup>

Relaxometry measurement on the  $\mu$ NMR systems was also applied to the detection of pathogens. Liong *et al.* reported a





**Fig. 4** Low-field  $\mu$ NMR. (A) 0.5 T permanent magnet ( $\phi$  8 cm  $\times$  H 5.5 cm, 1.25 kg). (B) Labeling procedure for the extravesicular markers and microfluidic system for on-chip detection of circulating human glioblastoma cell produced MVs.<sup>88</sup> (C) Setup (i and ii) and the transceiver (iii and iv) of the DMF-NMR relaxometer.<sup>92</sup> (D) An ODNP probe that fits inside a palm-sized permanent magnet for the hyperpolarization and detection of  $^1\text{H}$  NMR signals.<sup>49</sup> Reproduced with permission from ref. 88. Copyright 2012 Nature Publishing Group, ref. 92. Copyright 2015 RSC publishing, and ref. 49. 2021 Nature Publishing Group.

magnetic barcode assay for the genetic detection of *Mycobacterium tuberculosis* (*M. tuberculosis*) and the drug-resistance strains. They demonstrated a streamlined operation in the microfluidic chip, where the mycobacterial genes were PCR-amplified and captured on microspheres, the

spheres were labelled by magnetic nanoprobe, and the nanoprobe were analyzed by NMR.<sup>89</sup> The whole assay can be finished in 2.5 h for mechanically processed sputum samples. To detect malaria, Peng *et al.* reported an interesting strategy by analyzing the relaxometry of red blood

cells (RBCs) on a home-built, low-cost  $\mu$ NMR system.<sup>90</sup> Malaria parasites can convert large amounts of cellular hemoglobin into hemozoin crystallites, which induces significant changes in  $T_2$  of protons in RBCs and thus can be used as an indicator of “parasite load” in blood. By using <10  $\mu$ L of whole blood sample, a parasitemia level of fewer than 10 parasites per  $\mu$ L was identified within a few minutes.

The above studies were performed on  $\mu$ NMR systems with common microchannel-based devices for sampling. Digital microfluidic (DMF) devices that allow automatic operation of droplets can also be harnessed to build  $\mu$ NMR systems. To reduce human efforts during the sample analysis, Lei *et al.* reported a DMF-based  $\mu$ NMR platform for real-time detection of biomarkers.<sup>91</sup> The DMF device and the NMR coils were well designed to suit the limited inner volume of the magnet. The authors demonstrated a proof-of-concept study to show that the system can move the droplet automatically on the DMF device and realize the detection of a single target (*i.e.*, avidin) based on the measurement of  $T_2$ . To further improve the detection performance, Lei *et al.* reduced the  $\mu$ NMR system to a palm size and increased the sampling throughput by introducing the position-feedback module (Fig. 4C).<sup>92</sup> The system can process distinct samples and perform sequential  $\mu$ NMR experiments on them, realizing transport, mixing and analysis in 2.2 min. Therefore, this portable platform could serve as a useful tool in point-of-care testing.

As compact  $\mu$ NMR systems have low sensitivity in producing NMR signals, researchers are trying various strategies (*e.g.*, DNP) to overcome this limitation.<sup>49,93,94</sup> DNP was first proposed by Albert Overhauser,<sup>95</sup> which can transfer the large magnetic moment of electron spins under microwave (MW) irradiation to nuclear spins and thus enhance the NMR signal intensity by up to 2 orders of magnitude.<sup>96</sup> To explore the feasibility of Overhauser DNP (ODNP) for improving the sensitivity of a low-field NMR system, Korvink and co-workers developed a miniaturized probe head (including a MW resonator, a microfluidic chip, electrical shims and an RF transceiver coil) mounted inside a palm-sized permanent magnet (Fig. 4D).<sup>49</sup> As a proof-of-concept, the authors performed a group of basic  $^1\text{H}$  ODNP experiments and demonstrated that a signal enhancement of  $\sim 40$  fold was achieved in the detection of 130 nL of DI water. A chemical shift resolution of 0.7 ppm was obtained for a well shimmed ODNP-enhanced  $^1\text{H}$  spectrum. Therefore, this work suggests that a compact  $\mu$ NMR system could also be used in point-of-care applications based on spectrum analysis.

To sum up, compact  $\mu$ NMR systems that integrate microfluidics and relevant micro-circuits in a low-field permanent magnet provide researchers the convenience of using NMR to detect various biomolecules, pathogens and cells. This type of system has a small size and low-cost, and requires only a few microliters of sample with minimal preparation steps. Though the current detection methods mainly rely on measuring the transverse relaxation time, spectrum analysis might also be widely used in biochemical

applications based on the compact  $\mu$ NMR spectrometers with enhanced sensitivity.

## 4. Conclusion and perspectives

As a versatile analytical instrument in various fields, NMR technologies have been developed for decades. The above summarized advances suggest that  $\mu$ NMR has received increasing attention from the research community. By leveraging the great fluid controllability of microfluidics and the nondestructive analysis of NMR with atomic resolution,  $\mu$ NMR has shown great potential in the analysis of low-mass biochemical samples. In particular, the stripline-based  $\mu$ NMR offers an easy-to-use way by placing the microfluidic chip into the slit of the stripline coil and can produce high-resolution spectra or even dynamic tracking for minimal biochemical samples due to the utilization of the state-of-the-art commercial NMR instruments. The compact  $\mu$ NMR, in contrast, achieved a miniaturized system by integrating the portable magnet, electronics, detecting coil and microchip for fast and low-cost assays with microliter samples. In addition to these studies showing the online combination of microfluidics and NMR, actually there are several reports indicating that the offline combination of microfluidics and NMR can also serve as a promising strategy for biochemical analysis. In these studies, the microchips were used to perform sample pretreatment (*e.g.*, concentrate the target biomarker,<sup>97</sup> deliver target proteins to cells,<sup>98</sup> and prepare residual dipolar coupling media automatically<sup>99</sup>) ahead, which facilitated an efficient NMR analysis subsequently.

As summarized above,  $\mu$ NMR systems allow the detection of minimal samples in a non-invasive way at an atomic resolution, which is significantly advantageous over other analytical methods (such as microfluidics-based fluorescence systems,<sup>100</sup> Raman systems,<sup>101</sup> mass spectroscopy systems,<sup>102</sup> *etc.*). However, current  $\mu$ NMR systems also show apparent limitations in terms of simplicity, sensitivity, throughput and others. Consequently, there is a considerable need to develop new  $\mu$ NMR systems to enable easy sample processing, fast reaction monitoring, high-sensitivity, high-resolution and high-throughput analysis, and eventually biologically meaningful applications. Herein, we highlight several directions that could potentially advance further  $\mu$ NMR-based analysis.

It should be meaningful to introduce more functional units into the microfluidics device, to allow the  $\mu$ NMR to analyze more complex biological samples (*e.g.*, natural products).<sup>103</sup> Most current  $\mu$ NMR platforms used microchips only with simple functions, for example, mixing and observation. More integrated units for filtering, concentrating, isolation, sorting and others should facilitate a more efficient sample pretreatment and benefit the downstream NMR analysis, though this might require careful chip design and an additional liquid controlling system. In terms of promoting its wide application, it must be necessary for  $\mu$ NMR to be standardized, such as the micro-device size,

the fluid connection ports and controller, the probe, the relevant pulse sequence and others. Currently, most laboratories are developing their own strategy to perform  $\mu$ NMR analysis, and it could be difficult for researchers from other labs to use the developed platforms even on similar NMR instruments. We anticipate that the standardization of  $\mu$ NMR systems could benefit the community like common commercial NMR products.

It is also extremely important to improve the detection sensitivity of  $\mu$ NMR and the spectrum resolution. This could be reached by further tuning the coil that better matches the sample detection zone to achieve a better quality factor. Another more efficient way could be introducing appropriate hyperpolarization techniques (e.g., PHIP, DNP, and others) to significantly increase the detection sensitivity.<sup>104</sup> We also envision that the established  $\mu$ NMR systems in the future could provide more comprehensive information such as different nuclei including  $^1\text{H}$ ,  $^{13}\text{C}$ ,  $^{15}\text{N}$ ,  $^{19}\text{F}$  and  $^{31}\text{P}$ . Therefore,  $\mu$ NMR can be used not only for biomarker detection or small chemical molecule analysis, but also to determine the structure of different biomolecules.

In summary, the combination of microfluidics and NMR in high-field and low-field instruments offers us the capability to analyze minimal biochemical samples in a non-invasive mode. We foresee that  $\mu$ NMR detectors will ultimately become widely used in both laboratory and clinical settings.

## Author contributions

Zheyu Li: data curation and writing – original draft. Qingjia Bao: writing – review & editing. Chaoyang Liu: writing – review & editing. Ying Li: conceptualization, writing – review & editing, supervision, and funding acquisition. Yunhuang Yang: writing – review & editing, supervision, and funding acquisition. Maili Liu: supervision and funding acquisition.

## Conflicts of interest

The authors declare no conflict of interest.

## Acknowledgements

We gratefully acknowledge the financial support from the National Key R&D Program of China (2018YFA0704000), the National Natural Science Foundation of China (22174150, 21904139, 22074152, and 21921004), and the Chinese Academy of Sciences (Y9Y1041001 and YJKYYQ20170026).

## References

- 1 F. Bloch, *Phys. Rev.*, 1946, **70**, 460–474.
- 2 E. M. Purcell, H. C. Torrey and R. V. Pound, *Phys. Rev.*, 1946, **69**, 37–38.
- 3 S. Li, G. Lu, X. Fang, T. A. Ramelot, M. A. Kennedy, X. Zhou, P. Gong, X. Zhang, M. Liu, J. Zhu and Y. Yang, *Nucleic Acids Res.*, 2020, **48**, 432–444.
- 4 L. E. Kay, *J. Magn. Reson.*, 2005, **173**, 193–207.
- 5 D. Marion, *Mol. Cell. Proteomics*, 2013, **12**, 3006–3025.
- 6 C. Simmler, J. G. Napolitano, J. B. McAlpine, S. N. Chen and G. F. Pauli, *Curr. Opin. Biotechnol.*, 2014, **25**, 51–59.
- 7 B. Blümich, *TrAC, Trends Anal. Chem.*, 2016, **83**, 2–11.
- 8 M. Seifrid, G. N. M. Reddy, B. F. Chmelka and G. C. Bazan, *Nat. Rev. Mater.*, 2020, **5**, 910–930.
- 9 E. Ploetz, H. Engelke, U. Lächelt and S. Wuttke, *Adv. Funct. Mater.*, 2020, **30**, 1909062.
- 10 I. Speciale, A. Notaro, P. Garcia-Vello, F. Di Lorenzo, S. Armiento, A. Molinaro, R. Marchetti, A. Silipo and C. De Castro, *Carbohydr. Polym.*, 2022, **277**, 118885.
- 11 C. Gobl, T. Madl, B. Simon and M. Sattler, *Prog. Nucl. Magn. Reson. Spectrosc.*, 2014, **80**, 26–63.
- 12 K. Zia, T. Siddiqui, S. Ali, I. Farooq, M. S. Zafar and Z. Khurshid, *Eur. J. Dent.*, 2019, **13**, 124–128.
- 13 L. A. Colnago, Z. Wiesman, G. Pages, M. Musse, T. Monaretto, C. W. Windt and C. Rondeau-Mouro, *J. Magn. Reson.*, 2021, **323**, 106899.
- 14 C. Shyu, S. Chavez, I. Boileau and B. L. Foll, *Brain Sci.*, 2022, **12**, 918.
- 15 L. Breindel, D. S. Burz and A. Shekhtman, *J. Proteomics*, 2019, **191**, 202–211.
- 16 A. Kalfe, A. Telfah, J. Lambert and R. Hergenroder, *Anal. Chem.*, 2015, **87**, 7402–7410.
- 17 A. H. Emwas, R. Roy, R. T. McKay, L. Tenori, E. Saccenti, G. A. N. Gowda, D. Raftery, F. Alahmari, L. Jaremko, M. Jaremko and D. S. Wishart, *Metabolites*, 2019, **9**, 123.
- 18 Q. Qiu, *Front. Aging Neurosci.*, 2022, **14**, 903269.
- 19 M. S. Fox, J. M. Gaudet and P. J. Foster, *Magn. Reson. Insights*, 2015, **8**, 53–67.
- 20 A. B. Gunnarsdottir, C. V. Amanchukwu, S. Menkin and C. P. Grey, *J. Am. Chem. Soc.*, 2020, **142**, 20814–20827.
- 21 M. Elsayed, A. Isah, M. Hiba, A. Hassan, K. Al-Garadi, M. Mahmoud, A. El-Husseiny and A. E. Radwan, *J. Pet. Explor. Prod.*, 2022, **12**(10), 2747–2784.
- 22 A. K. Mittermaier and L. E. Kay, *Trends Biochem. Sci.*, 2009, **34**, 601–611.
- 23 K. Hashi, S. Ohki, S. Matsumoto, G. Nishijima, A. Goto, K. Deguchi, K. Yamada, T. Noguchi, S. Sakai, M. Takahashi, Y. Yanagisawa, S. Iguchi, T. Yamazaki, H. Maeda, R. Tanaka, T. Nemoto, H. Suematsu, T. Miki, K. Saito and T. Shimizu, *J. Magn. Reson.*, 2015, **256**, 30–33.
- 24 S. Li, G. Lu, X. Fang, T. A. Ramelot, M. A. Kennedy, X. Zhou, P. Gong, X. Zhang, M. Liu, J. Zhu and Y. Yang, *Nucleic Acids Res.*, 2020, **48**, 432–444.
- 25 J. M. Aramini, P. Rossi, C. Anklin, R. Xiao and G. T. Montelione, *Nat. Methods*, 2007, **4**, 491–493.
- 26 D. L. Olson, J. A. Norcross, M. O'Neil-Johnson, P. F. Molitor, D. J. Detlefsen, A. G. Wilson and T. L. Peck, *Anal. Chem.*, 2004, **76**, 2966–2974.
- 27 D. L. Olson, T. L. Peck, A. G. Webb, R. L. Magin and J. V. Sweedler, *Science*, 1995, **270**, 1967–1970.
- 28 J. Deng, K. Wang, M. Wang, P. Yu and L. Mao, *J. Am. Chem. Soc.*, 2017, **139**, 5877–5882.



- 29 S. S. Zaleskiy, E. Danieli, B. Blumich and V. P. Ananikov, *Chem. Rev.*, 2014, **114**, 5641–5694.
- 30 S. Battat, D. A. Weitz and G. M. Whitesides, *Lab Chip*, 2022, **22**, 530–536.
- 31 S. Haeberle and R. Zengerle, *Lab Chip*, 2007, **7**, 1094–1110.
- 32 G. Yesiloz, M. S. Boybay and C. L. Ren, *Anal. Chem.*, 2017, **89**, 1978–1984.
- 33 Y. Li, Y. Xu, X. Feng and B. F. Liu, *Anal. Chem.*, 2012, **84**, 9025–9032.
- 34 Y. Li, P. Zhang, T. Li, R. Hu, J. Zhu, T. He, Y. Yang and M. Liu, *Sens. Actuators, B*, 2020, **308**, 127749.
- 35 N. Frey, U. M. Sonmez, J. Minden and P. LeDuc, *Nat. Commun.*, 2022, **13**, 3195.
- 36 C. H. Choi, S. M. Hong, J. Felder and N. J. Shah, *Magn. Reson. Imaging*, 2020, **72**, 103–116.
- 37 J. H. Lee, Y. Okuno and S. Cavagnero, *J. Magn. Reson.*, 2014, **241**, 18–31.
- 38 A. Webb, *Anal. Chem.*, 2012, **84**, 9–16.
- 39 A. P. Kentgens, J. Bart, P. J. van Bentum, A. Brinkmann, E. R. van Eck, J. G. Gardeniers, J. W. Janssen, P. Knijn, S. Vasa and M. H. Verkuijlen, *J. Chem. Phys.*, 2008, **128**, 052202.
- 40 H. Lee, E. Sun, D. Ham and R. Weissleder, *Nat. Med.*, 2008, **14**, 869–874.
- 41 J. B. Haun, C. M. Castro, R. Wang, V. M. Peterson, B. S. Marinelli, H. Lee and R. Weissleder, *Sci. Transl. Med.*, 2011, **3**, 71ra16.
- 42 C. M. Castro, A. A. Ghazani, J. Chung, H. Shao, D. Issadore, T. J. Yoon, R. Weissleder and H. Lee, *Lab Chip*, 2014, **14**, 14–23.
- 43 A. Dupré, K.-M. Lei, P.-I. Mak, R. P. Martins and W. K. Peng, *Microelectron. Eng.*, 2019, **209**, 66–74.
- 44 J. Guo, D. Jiang, S. Feng, C. Ren and J. Guo, *Electrophoresis*, 2020, **41**, 319–327.
- 45 M. Grisi, G. Gualco and G. Boero, *Rev. Sci. Instrum.*, 2017, **86**, 044703.
- 46 H. D. Phuc, Development of portable low field NMR magnet: Design and construction, *PhD thesis*, INSA de Lyon, 2015.
- 47 C. Hierold, G. K. Fedder, J. G. Korvink, J. A. Oliver and B. O. Tabata, *Micro and Nano Scale NMR: Technologies and Systems*, John Wiley and Sons, 2018.
- 48 K.-M. Lei, H. Heidari, P.-I. Mak, M.-K. Law, F. Maloberti and R. P. Martins, *IEEE J. Solid-State Circuits*, 2017, **52**, 284–297.
- 49 S. Z. Kiss, N. MacKinnon and J. G. Korvink, *Sci. Rep.*, 2021, **11**, 4671.
- 50 A. Yilmaz and M. Utz, *Lab Chip*, 2016, **16**, 2079–2085.
- 51 C. Massin, F. Vincent, A. Homsy, K. Ehrmann, G. Boero, P. A. Besse, A. Daridon, E. Verpoorte, N. F. de Rooij and R. S. Popovic, *J. Magn. Reson.*, 2003, **164**, 242–255.
- 52 P. J. van Bentum, J. W. Janssen, A. P. Kentgens, J. Bart and J. G. Gardeniers, *J. Magn. Reson.*, 2007, **189**, 104–113.
- 53 D. E. Bordelon, R. C. Goldstein, V. S. Nemkov, A. Kumar, J. K. Jackowski, T. L. DeWeese and R. Ivkov, *IEEE Trans. Magn.*, 2012, **48**, 47–52.
- 54 E. E. McDonnell, S. Han, C. Hilty, K. L. Pierce and A. Pines, *Anal. Chem.*, 2005, **77**, 8109–8114.
- 55 S. Han, J. Granwehr, S. Garcia, E. E. McDonnell and A. Pines, *J. Magn. Reson.*, 2006, **182**, 260–272.
- 56 R. C. Meier, J. Höfflin, V. Badilita, U. Wallrabe and J. G. Korvink, *J. Micromech. Microeng.*, 2014, **24**, 045021.
- 57 M. Mompeán, R. M. Sanchez-Donoso, A. de la Hoz, V. Saggiomo, A. H. Velders and M. V. Gomez, *Nat. Commun.*, 2018, **9**, 108.
- 58 R. M. Fratila, M. V. Gomez, S. Sykora and A. H. Velders, *Nat. Commun.*, 2014, **5**, 3025.
- 59 V. Esteve, J. Berganzo, R. Monge, M. C. Martinez-Bisbal, R. Villa, B. Celda and L. Fernandez, *Biomechanics*, 2014, **8**, 064105.
- 60 L. Bordonali, N. Nordin, E. Fuhrer, N. MacKinnon and J. G. Korvink, *Lab Chip*, 2019, **19**, 503–512.
- 61 J. Li and C. C. Kim, *Lab Chip*, 2020, **20**, 1705–1712.
- 62 C. H. Ooi, R. Vadivelu, J. Jin, K. R. Sreejith, P. Singha, N. K. Nguyen and N. T. Nguyen, *Lab Chip*, 2021, **21**, 1199–1216.
- 63 I. Swyer, S. von der Ecken, B. Wu, A. Jenne, R. Soong, F. Vincent, D. Schmidig, T. Frei, F. Busse, H. J. Stronks, A. J. Simpson and A. R. Wheeler, *Lab Chip*, 2019, **19**, 641–653.
- 64 B. Wu, S. von der Ecken, I. Swyer, C. Li, A. Jenne, F. Vincent, D. Schmidig, T. Kuehn, A. Beck, F. Busse, H. Stronks, R. Soong, A. R. Wheeler and A. Simpson, *Angew. Chem., Int. Ed.*, 2019, **58**, 15372–15376.
- 65 J. Bart, A. J. Kolkman, A. J. O.-d. Vries, K. Koch, P. J. Nieuwland, H. J. W. G. Janssen, J. P. J. M. van Bentum, K. A. M. Ampt, F. P. J. T. Rutjes, S. S. Wijmenga, H. J. G. E. Gardeniers and A. P. M. Kentgens, *J. Am. Chem. Soc.*, 2008, **131**, 5014–5015.
- 66 A. J. Oosthoek-de Vries, J. Bart, R. M. Tiggelaar, J. W. Janssen, P. J. van Bentum, H. J. Gardeniers and A. P. Kentgens, *Anal. Chem.*, 2017, **89**, 2296–2303.
- 67 S. G. J. van Meerten, P. J. M. van Bentum and A. P. M. Kentgens, *Anal. Chem.*, 2018, **90**, 10134–10138.
- 68 A. J. Oosthoek-de Vries, P. J. Nieuwland, J. Bart, K. Koch, J. W. G. Janssen, P. J. M. van Bentum, F. Rutjes, H. Gardeniers and A. P. M. Kentgens, *J. Am. Chem. Soc.*, 2019, **141**, 5369–5380.
- 69 S. van Meerten, F. van Zelst, K. Tijssen and A. Kentgens, *Anal. Chem.*, 2020, **92**, 13010–13016.
- 70 G. Finch, A. Yilmaz and M. Utz, *J. Magn. Reson.*, 2016, **262**, 73–80.
- 71 W. L. Robb, *Ann. N. Y. Acad. Sci.*, 1968, **146**, 119–137.
- 72 B. Patra, M. Sharma, W. Hale and M. Utz, *Sci. Rep.*, 2021, **11**, 53.
- 73 M. Plata, W. Hale, M. Sharma, J. M. Werner and M. Utz, *Lab Chip*, 2021, **21**, 1598–1603.
- 74 Y. Zhuo, X. Wang, S. Chen, H. Chen, J. Ouyang, L. Yang, X. Wang, L. You, M. Utz, Z. Tian and X. Cao, *Chemistry*, 2021, **27**, 9508–9513.
- 75 Y. Sun, H. Fang, X. Lin, X. Wang, G. Chen, X. Wang, Z. Tian, L. Yang, M. Utz and X. Cao, *CCS Chem.*, 2022, **4**, 557–565.

- 76 S. J. Barker, L. Dagys, W. Hale, B. Ripka, J. Eills, M. Sharma, M. H. Levitt and M. Utz, *Anal. Chem.*, 2022, **94**, 3260–3267.
- 77 T. R. Alderson and L. E. Kay, *Cell*, 2021, **184**, 577–595.
- 78 E. F. Dudas and A. Bodor, *Anal. Chem.*, 2019, **91**, 4929–4933.
- 79 R. Lu, H. Yi, W. Wu and Z. Ni, *Chin. J. Mech. Eng.*, 2013, **26**, 689–694.
- 80 N. Sun, T.-J. Yoon, H. Lee, W. Andress, R. Weissleder and D. Ham, *IEEE J. Solid-State Circuits*, 2011, **46**, 342–352.
- 81 A. A. Ghazani, S. McDermott, M. Pectasides, M. Sebas, M. Mino-Kenudson, H. Lee, R. Weissleder and C. M. Castro, *Nanomedicine*, 2013, **9**, 1009–1017.
- 82 H. J. Chung, C. M. Castro, H. Im, H. Lee and R. Weissleder, *Nat. Nanotechnol.*, 2013, **8**, 369–375.
- 83 L. Josephson, J. M. Perez and R. Weissleder, *Angew. Chem., Int. Ed.*, 2001, **40**, 3204–3206.
- 84 H. Shao, C. Min, D. Issadore, M. Liong, T. J. Yoon, R. Weissleder and H. Lee, *Theranostics*, 2012, **2**, 55–65.
- 85 J. M. Perez, L. Josephson, T. O'Loughlin, D. Högemann and R. Weissleder, *Nat. Biotechnol.*, 2002, **20**, 816–820.
- 86 R. Lu, P. Lei, Q. Yang, Z. Ni and H. Yi, *Appl. Magn. Reson.*, 2018, **50**, 357–370.
- 87 H. Lee, T.-J. Yoon, J.-L. Figueiredo, F. K. Swirski and R. Weissleder, *Proc. Natl. Acad. Sci. U. S. A.*, 2009, **106**, 12459–12464.
- 88 H. Shao, J. Chung, L. Balaj, A. Charest, D. D. Bigner, B. S. Carter, F. H. Hochberg, X. O. Breakefield, R. Weissleder and H. Lee, *Nat. Med.*, 2012, **18**, 1835–1840.
- 89 M. Liong, A. N. Hoang, J. Chung, N. Gural, C. B. Ford, C. Min, R. R. Shah, R. Ahmad, M. Fernandez-Suarez, S. M. Fortune, M. Toner, H. Lee and R. Weissleder, *Nat. Commun.*, 2013, **4**, 1752.
- 90 W. K. Peng, T. F. Kong, C. S. Ng, L. Chen, Y. Huang, A. A. Bhagat, N. T. Nguyen, P. R. Preiser and J. Han, *Nat. Med.*, 2014, **20**, 1069–1073.
- 91 K. M. Lei, P. I. Mak, M. K. Law and R. P. Martins, *Analyst*, 2014, **139**, 6204–6213.
- 92 K. M. Lei, P. I. Mak, M. K. Law and R. P. Martins, *Analyst*, 2015, **140**, 5129–5137.
- 93 N. Sahin Solmaz, M. Grisi, A. V. Matheoud, G. Gualco and G. Boero, *Anal. Chem.*, 2020, **92**, 9782–9789.
- 94 V. Badilita, R. C. Meier, N. Spengler, U. Wallrabe, M. Utz and J. G. Korvink, *Soft Matter*, 2012, **8**, 10583–10597.
- 95 A. W. Overhauser, *Phys. Rev.*, 1953, **92**, 411–415.
- 96 J. H. Ardenkjaer-Larsen, *J. Magn. Reson.*, 2016, **264**, 3–12.
- 97 T. F. Kong, W. Ye, W. K. Peng, H. W. Hou, Marcos, P. R. Preiser, N. T. Nguyen and J. Han, *Sci. Rep.*, 2015, **5**, 11425.
- 98 N. Sciolino, A. Liu, L. Breindel, D. S. Burz, T. Sulchek and A. Shekhtman, *Commun. Biol.*, 2022, **5**, 451.
- 99 Z. Li, Y. Xiong, S. Li, J. Zhu, R. Hu, Y. Li, Y. Yang and M. Liu, *Chem. Eng. J.*, 2022, **431**, 133817.
- 100 Z. Guo, H. Cheng, Z. Li, S. Shao, P. Sarkar, S. Wang, R. Chaudhuri, N. G. Perkins, F. Ji, W. Wei and M. Xue, *J. Am. Chem. Soc.*, 2021, **143**, 11191–11198.
- 101 T. M. Watanabe, K. Sasaki and H. Fujita, *Genes*, 2022, **13**, 2127.
- 102 R. Hu, Y. Li, Y. Yang and M. Liu, *Mass Spectrom. Rev.*, 2023, **42**, 67–94.
- 103 R. Ueoka, P. Sondermann, S. Leopold-Messer, Y. Liu, R. Suo, A. Bhushan, L. Vadakumchery, U. Greczmiel, Y. Yashiroda, H. Kimura, S. Nishimura, Y. Hoshikawa, M. Yoshida, A. Oxenius, S. Matsunaga, R. T. Williamson, E. M. Carreira and J. Piel, *Nat. Chem.*, 2022, **14**(10), 1193–1201.
- 104 J. Eills, W. Hale and M. Utz, *Prog. Nucl. Magn. Reson. Spectrosc.*, 2022, **128**, 44–69.